pH-Responsive Micellization of Amphiphilic Diblock Copolymers Synthesized via Reversible Addition−Fragmentation Chain Transfer Polymerization

Shin-ichi Yusa,*,† Yoshihiko Shimada,† Yoshiro Mitsukami,‡ Tohei Yamamoto,† and Yotaro Morishima§

Department of Applied Chemistry, Himeji Institute of Technology, 2167 Shosha, Himeji 671-2201, Japan; Department of Macromolecular Science, Graduate School of Science, Osaka University, Toyonaka 560-0043, Japan, and Faculty of Engineering, Fukui University of Technology, 6-3-1 Gakuen, Fukui 910-8505, Japan

Received January 27, 2003; Revised Manuscript Received April 8, 2003

ABSTRACT: Well-defined poly(sodium 2-(acrylamido)-2-methylpropanesulfonate-*block*-sodium 6-acrylamidohexanoate) (pNaAMPS-AaH) was synthesized by reversible addition−fragmentation chain transfer (RAFT) radical polymerization of sodium 6-acrylamidohexanoate (AaH) using the sodium 2-(acrylamido)-2-methylpropanesulfonate-based macrochain transfer agent. The "living" polymerization of AaH was evidenced by the fact that the number-average molecular weight increased linearly with monomer conversion while the molecular weight distribution remained narrow independent of the conversion. pH-induced association and dissociation behavior of the diblock copolymers was investigated by quasi-elastic light scattering (QELS), static light scattering (SLS), ^{1}H NMR spin−spin relaxation time, and fluorescence probe techniques. At pH < 4, the diblock copolymers exhibited large values of the hydrodynamic radius and small values of the ^{1}H NMR spin−spin relaxation time. These observations indicated that micellization occurred to form polymer micelles comprising hydrophobic protonated AaH cores and hydrophilic NaAMPS coronas at pH < 4. On the other hand, these diblock copolymers dissolved in aqueous solutions as a state of unimer under high-pH conditions. 8-Anilino-1-naphthalenesulfonic acid, ammonium salt hydrate (ANS), as a fluorescence probe could be incorporated into the protonated AaH core of diblock copolymer micelles at low pH and released upon dissociation of the micelles at high pH, which was completely reversible.

Introduction

Amphiphilic diblock copolymers form micelles in aqueous solutions in which hydrophobic blocks constitute cores and hydrophilic blocks form coronas. The amphiphilic block copolymer micelles are important in many applications, including separation[1] and delivery systems.[2] In recent years, external stimuli-responsive block copolymers have attracted considerable interest. Remarkable progress has been made in the development of block copolymers responding to physical and chemical stimuli such as heat, changes in pH, and added electrolyte.[3−5]

Progress in polymer synthesis techniques makes it possible to produce various water-soluble block copolymers with controlled structures. Radical polymerization methods that have been used to synthesize well-defined polymers include nitroxide-mediated or stable free radical polymerization (SFRP),[6] atom transfer radical polymerization (ATRP),[7,8] and reversible addition−fragmentation chain transfer (RAFT) methods.[9] Above them, the advantage of RAFT polymerization is applicable to a wide range of monomers under a broad range of experimental conditions. A number of external stimuli-responsive block copolymers have been synthesized via the RAFT process. For example, using sequential free radical polymerization via the RAFT process, Laschewsky and co-workers[10] synthesized switchable block copolymers with double thermoresponsivity, containing two blocks, one presenting a lower critical solution temperature (LCST) and the other an upper critical solution temperature (UCST). McCormick and co-workers[11] synthesized poly(sodium 4-styrenesulfonate-*block*-sodium 4-vinylbenzoate) (pNaSS-VB) via RAFT radical polymerization. Armes and co-workers[12] synthesized pNaSS-VB with varying VB contents via 2,2,6,6-tetramethylpiperidinyl-1-oxy (TEMPO)-mediated living radical polymerization. These pNaSS-VB diblock copolymers undergo reversible pH-induced micellization in aqueous solutions, forming the hydrophobic micellar core of the carboxylic acid blocks. From quasi-elastic light scattering (QELS) studies, it was revealed that pNaSS-VB forms polymer micelles with a hydrodynamic diameter of 20 nm at pH 3.9.[12]

In this paper, we report on the controlled synthesis of diblock copolymers of sodium 2-(acrylamido)-2-methylpropanesulfonate (NaAMPS) and sodium 6-acrylamidohexanoate (AaH) in aqueous solutions by the RAFT process using the NaAMPS macrochain transfer agent (Chart 1). This diblock copolymer exhibits pH-induced self-association due to selective protonation of the carboxylate residues at low pH's. We mainly focused on the pH-responsive association and dissociation behavior of the diblock copolymers in aqueous solutions as characterized using QELS, static light scattering (SLS), ^{1}H NMR relaxation time, and fluorescence probe techniques.

Experimental Section

Reagents. 4-Cyanopentanoic acid dithiobenzoate was synthesized according to the method reported by McCormick and

† Himeji Institute of Technology.
‡ Osaka University.
§ Fukui University of Technology.
* To whom correspondence should be addressed. E-mail: yusa@chem.eng.himeji-tech.ac.jp.

10.1021/ma030065x CCC: $25.00
Published on Web 05/06/2003

Chart 1. Diblock Copolymer Used in This Study

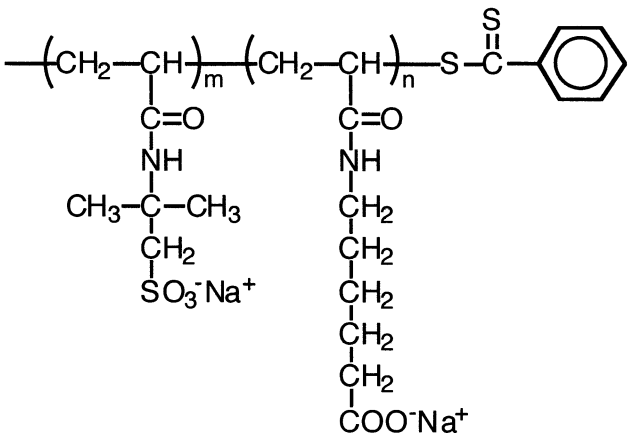

pNaAMPS–AaH

co-workers.[11] Sodium 6-acrylamidohexanoate (AaH) was prepared as reported previously.[13] Methanol was dried over 4 Å molecular sieves and distilled. Water was purified with a Millipore Milli-Q system. Other reagents were used as received.

Preparation of NaAMPS Macro-Chain Transfer Agent. A representative example for the preparation of NaAMPS macro-chain transfer agent (macro-CTA) is as follows. 2-(Acrylamido)-2-methylpropanesulfonic acid (AMPS) (25.0 g, 121 mmol) was neutralized with NaOH (4.81 g, 121 mmol) in 60 mL of water, and 4-cyanopentanoic acid dithiobenzoate (232 mg, 0.829 mmol) and 4,4′-azobis(4-cyanopentanoic acid) (46.4 mg, 0.166 mmol) were added to this solution. The mixture was degassed by purging with Ar gas for 30 min. Polymerization was carried out at 70 °C for 4 h. The polymer was dialyzed against pure water for a week and recovered by a freeze-drying technique (conversion 83.9%). The obtained NaAMPS polymer could be used as a macro-CTA.

Block Copolymerization. A typical procedure for block copolymerization is as follows. NaAMPS macro-CTA (2.70 g), AaH (1.70 g, 8.23 mmol), and 4,4′-azobis(4-cyanopentanoic acid) (5.1 mg, 0.018 mmol) were dissolved in 15 mL of water. The solution was deoxygenated by purging with Ar gas for 30 min. Block copolymerization was carried out at 70 °C for 4 h. The diblock copolymer was purified by dialysis against a dilute NaOH aqueous solution (pH 8) for a week, changing the dilute alkaline aqueous solution twice a day. The diblock copolymer was recovered by a freeze-drying technique. Gel permeation chromatography (GPC) for the reaction mixture was measured to estimate the molecular weight and molecular weight distribution (M_w/M_n). To investigate the relationship between polymerization time and conversion, the conversion was determined by ^{1}H NMR spectroscopy. Predetermined amounts of AaH, NaAMPS macro-CTA, and initiator were dissolved in D_2O. The solution was added to an NMR tube and deoxygenated by purging with Ar gas for 30 min. After deoxygenation, the cap was sealed and the tube placed in the temperature-equilibrated (70 °C) probe of a NMR spectrometer.

Measurements. Gel Permeation Chromatography (GPC). GPC analysis were performed at 40 °C with a JASCO GPC-900 equipped with a JASCO UV-975 UV/vis detector and two Tosoh TSKgel α-M columns using a 0.1 M $NaNO_3$ aqueous solution containing 20 vol % acetonitrile as an eluent at a flow rate of 1.0 mL/min. The GPC detectors included refractive index (RI) and ultraviolet (UV) absorption at 304 nm. The number-average molecular weight (M_n), weight-average molecular weight (M_w), and M_w/M_n of the sample polymers were calibrated with standard sodium poly(styrenesulfonate) samples of 11 different molecular weights ranging from 1.37×10^3 to 2.61×10^6.

Quasi-Elastic Light Scattering (QELS). QELS data were obtained at 25 °C with an Otsuka Electronics Photal DLS-7000DL light scattering spectrometer equipped with an ALV-5000E multi-τ digital time correlator. An Ar^+ laser (50.0 mW at 488 nm) was used as a light source.

The intensity−intensity time correlation $g^{(2)}(t)$ in the self-beating mode was measured, and $g^{(2)}(t)$ is related to the normalized autocorrelation function of the scattered electric field $g^{(1)}(t)$:

$$g^{(2)}(t) = B(1 + \beta|g^{(1)}(t)|^2) \quad (1)$$

where B is a baseline, β is a factor which takes into account deviations from ideal correlation, and t is the delay time. For a polydisperse sample, $g^{(1)}(t)$ is related to the relaxation time distribution, $\tau A(\tau)$. To obtain $\tau A(\tau)$, the inverse Laplace transform (ILT) analysis was performed using a constrained regularization routine, REPES.[14,15]

$$g^{(1)}(t) = \int \tau A(\tau) \exp(-t/\tau)\, \mathrm{d} \ln \tau \quad (2)$$

Here, τ is the relaxation time. The relaxation time distributions are given as a $\tau A(\tau)$ vs log τ profile with an equal area. The translational diffusion coefficient (D) is calculated from $D = (\Gamma/q^2)_{q\to 0}$, where Γ is the relaxation rate and $q = (4\pi n/\lambda) \sin(\theta/2)$ with n being the refractive index of solvent, λ being the wavelength (= 488 nm), and θ being the scattering angle. The hydrodynamic radius (R_h) is calculated using the Einstein−Stokes relation $R_h = k_B T/6\pi\eta D$, where k_B is Boltzmann's constant, T is the absolute temperature, and η is the solvent viscosity.

Static Light Scattering (SLS). SLS measurements were performed at 25 °C with an Otsuka Electronics Photal DLS-7000DL light scattering spectrometer equipped with an Ar^+ laser (50.0 mW at 488 nm). M_w, z-average radius of gyration (R_g), and the second virial coefficient (A_2) values were estimated from the relation[16]

$$\frac{KC_p}{R_\theta} = \frac{1}{M_w}\left(1 + \frac{1}{3}\langle R_g^2\rangle q^2\right) + 2A_2C_p \quad (3)$$

where C_p is the polymer concentration, R_θ is the Rayleigh ratio, and $K = 4\pi^2 n^2 (\mathrm{d}n/\mathrm{d}C_p)^2/N_A\lambda^4$ with $\mathrm{d}n/\mathrm{d}C_p$ being the refractive index increment against C_p and N_A being Avogadro's number. By measuring R_θ for a set of C_p and θ, values of M_w, R_g, and A_2 were estimated from Zimm plots. Benzene was used for the calibration of the instrument. Values of $\mathrm{d}n/\mathrm{d}C_p$ were determined with an Otsuka Electronics Photal DRM-1020 differential refractometer at 25 °C.

^{1}H NMR Relaxation Time. ^{1}H NMR spectra were obtained with a Bruker DRX-500 spectrometer operating at 500 MHz in D_2O. Chemical shifts were determined by using 3-(trimethylsilyl)propionic-2,2,3,3-d_4 acid as an internal reference. ^{1}H NMR spin−spin relaxation times (T_2) were determined by the Carr−Purcell−Meiboom−Gill (CPMG) method.[17] A 90° pulse of 13.85 μs was calibrated and used for the measurement. Peak intensities at 12 different numbers of the 180° pulse were measured.

Fluorescence. Fluorescence spectra were recorded on a Hitachi F-2500 fluorescence spectrophotometer. 8-Anilino-1-naphthalenesulfonic acid, ammonium salt hydrate (ANS), was used as a fluorescence probe. A 0.1 M NaCl aqueous stock solution of ANS (1.89×10^{-4} M) was prepared. Emission spectra of ANS were measured with excitation at 350 nm. Excitation and emission slit widths were maintained at 20 and 5.0 nm, respectively.

Preparation of Sample Solutions. The solution pH was adjusted by adding a proper amount of aqueous NaOH or HCl. All measurements were made with 0.1 M NaCl aqueous solutions to avoid an effect of a small change in the ion strength resulting from a small amount of NaOH or HCl added to the solutions. For QELS measurements, polymer solutions containing 0.1 M NaCl were employed to minimize interpolymer electrostatic interactions. The polymer concentration was 10 g/L. SLS and $\mathrm{d}n/\mathrm{d}C_p$ measurements were performed at C_p ranging from 1.0 to 10 g/L in 0.1 M NaCl. Sample solutions

for QELS and SLS measurements were filtered with a 0.2 μm pore size membrane filter. The sample solutions of the diblock copolymers at C_p = 10 g/L for ^{1}H NMR measurements were prepared in D_2O containing 0.1 M NaCl, and pD was adjusted with a D_2O solution of NaOD or DCl. The final pD value was determined from the relation pD = pH + 0.4.[18]

Results and Discussion

Synthesis of NaAMPS−AaH Diblock Copolymers. We performed polymerization of NaAMPS by RAFT in aqueous solution at pH 7.5 following papers by McCormick and co-workers[19] who reported RAFT polymerization of NaAMPS proceeded in a "living" fashion in aqueous media. 4,4′-Azobis(4-cyanopentanoic acid) and 4-cyanopentanoic acid dithiobenzoate were used as an initiator and as a chain transfer agent (CTA), respectively with a molar ratio maintained at 1/5. The monomer concentration was 2.0 M. The M_n value of the polymer obtained was 1.91×10^4 with an M_w/M_n ratio of 1.26. Values of M_n and M_w/M_n for polymers obtained in a control experiment, where no CTA was added, were found to be 2.10×10^5 and 9.67, respectively. These results imply that the polymerization of NaAMPS by RAFT proceeds in a "living" manner with a dithioester moiety at one chain end and thus the yielded could be used as a macro-CTA.

In Figure 1a, a time−conversion relationship is depicted along with the first-order kinetic plot for the polymerization of AaH in the presence of NaAMPS macro-CTA ($M_n = 1.91 \times 10^4$; $M_w/M_n = 1.26$) and 4,4′-azobis(4-cyanopentanoic acid) at 70 °C in D_2O under an Ar atmosphere. The monomer consumption was monitored by ^{1}H NMR spectroscopy as a function of time. There was an induction period of 13 min, which may be due to a slow rate of the formation of the 4-cyanopentanoic acid radical fragment. A monomer conversion of 86% was reached after 240 min. The kinetic plot for RAFT polymerization deviated significantly from the first-order kinetics. The breakdown in the "livingness" of the polymerization, like other controlled free radical processes, is indicative of the presence of bimolecular termination events.[20,21] Similar observations of a induction period early in the polymerization and deviation from the first-order kinetics above 55% conversion were reported by McCormick and co-workers[21] for the RAFT polymerization of *N*,*N*-dimethylacrylamide (DMA) in benzene at 60 °C using 2,2′-azobis(isobutyronitrile) as an initiator at a CTA/initiator ratio of 5/1.

In Figure 1b, a GPC elution curve (RI response) for the NaAMPS and AaH diblock copolymer sample (pNaAMPS-AaH) is compared with that for the NaAMPS macro-CTA before block copolymerization. A significant increase in the molecular weight occurs upon polymerization of AaH in the presence of the NaAMPS macro-CTA. Neither a new peak nor a shoulder due to AaH homopolymers formed by homopolymerization was observed. The polymers formed by the RAFT process show UV absorption at 304 nm due to the $\pi-\pi^*$ transition of a dithiobenzoate moiety at the polymer chain end. GPC elution traces detected by UV absorption at 304 nm were virtually the same as those detected by RI.

In Figure 1c, values of M_n and M_w/M_n estimated from GPC for the diblock copolymers in the polymerization of AaH in the presence of the NaAMPS macro-CTA ($M_n = 1.91 \times 10^4$; $M_w/M_n = 1.26$) are plotted as a function of the conversion of AaH determined by ^{1}H NMR. The M_n value increases almost linearly with the conversion while M_w/M_n remains nearly constant ($M_w/M_n < 1.32$)

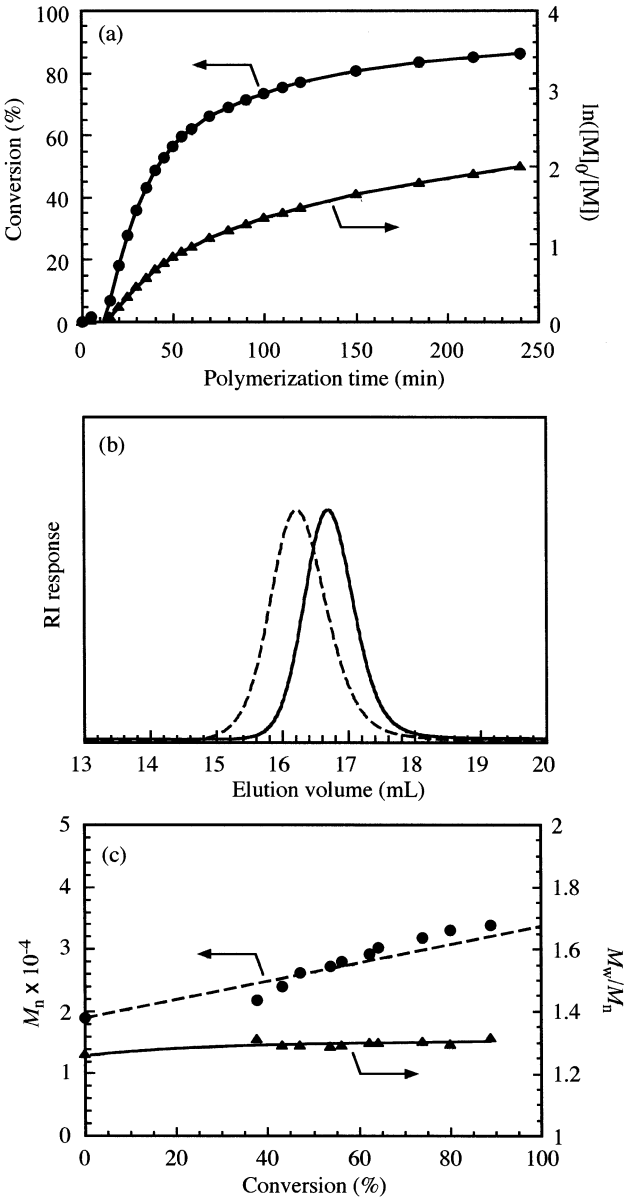

Figure 1. (a) Time−conversion and the first-order kinetic plots for the polymerization of AaH in the presence of NaAMPS macro-CTA in D_2O at 70 °C. (b) GPC elution curves for a sample of NaAMPS macro-CTA ($M_n = 1.91 \times 10^4$; $M_w/M_n = 1.26$) (—) and corresponding diblock copolymer of NaAMPS and AaH ($M_n = 3.39 \times 10^4$; $M_w/M_n = 1.32$) (- - -). (c) Dependence of M_n and M_w/M_n on the monomer conversion in the polymerization of AaH in the presence of NaAMPS macro-CTA in D_2O at 70 °C. The broken line represents the theoretical line.

independent of the conversion. All the values of M_n are close to the theoretical values predicted for a living mechanism.

The same NaAMPS macro-CTA of $M_n = 1.91 \times 10^4$ was used to prepare a series of NaAMPS-AaH diblock copolymers with different AaH block lengths. Degrees of polymerization (DP) for NaAMPS and AaH blocks were calculated from GPC and ^{1}H NMR, respectively. Table 1 lists molecular parameters for the diblock copolymers together with M_n and M_w/M_n values estimated by GPC.

Quasi-Elastic Light Scattering (QELS). The formation of polymer micelles from the diblock copolymers under acidic conditions was observed by QELS. Relaxation time distributions at pH 3 and 9 were measured

Table 1. Molecular Weights and Compositions of the Diblock Copolymers

sample code	DP of NaAMPS block [a]	DP of AaH block[b]	M_n[a] $\times 10^{-4}$	M_w/M_n[a]
$pNaAMPS_{85}-AaH_{30}$	85	30	3.02	1.21
$pNaAMPS_{85}-AaH_{40}$	85	40	3.12	1.25

[a] Degrees of polymerization (DP) were determined by GPC eluted with a mixed solvent of water and acetonitrile (80/20, v/v) containing 0.1 M $NaNO_3$. [b] Estimated by ^1H NMR.

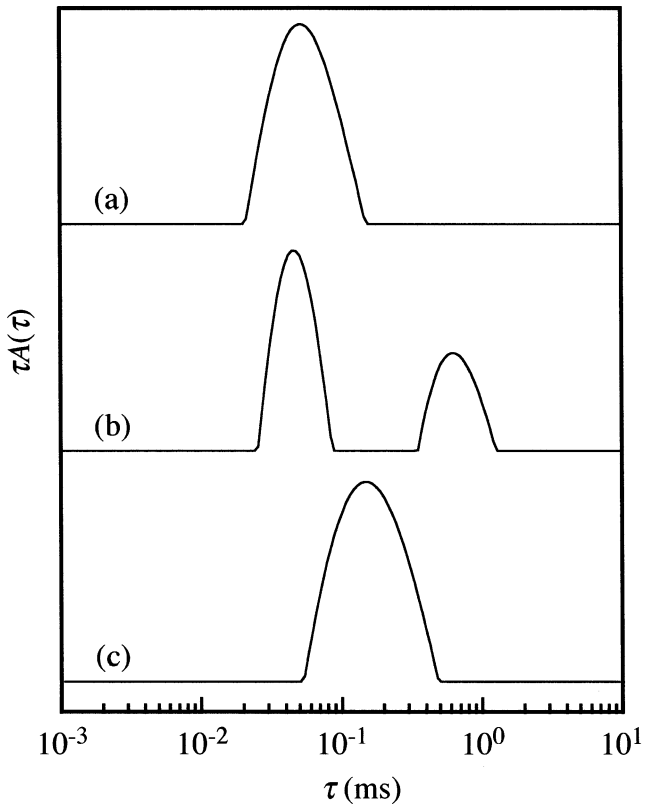

Figure 2. Typical examples of QELS relaxation time distributions for $pNaAMPS_{85}-AaH_{40}$ at $C_p = 10$ g/L in 0.1 M NaCl aqueous solutions at pH 9 (a), 5 (b), and 3 (c) at $\theta = 90°$.

at different scattering angles (30°, 50°, 70°, 90°, 110°, and 130°) at $C_p = 10$ g/L, and the relaxation rate (Γ) at each peak top was plotted against the square of the scattering vector (q^2) (data not shown). These plots yielded a straight line passing through the origin. Thus, the observed relaxation times are attributed to a diffusive mode. Values of D estimated from the slope of the $\Gamma-q^2$ plots were found to be in good agreement with those calculated from Γ at the peak top of the relaxation time distribution obtained at a fixed θ of 90°. Therefore, we used D values calculated from Γ at the peak top. The R_h values were estimated from the Einstein−Stokes equation using the D values. Figure 2 compares QELS relaxation time distributions for $pNaAMPS_{85}$-AaH_{40} at varying pH in 0.1 M NaCl aqueous solutions at $C_p = 10$ g/L observed at a θ of 90°. The distributions are unimodal at pH 9 and 3 with different relaxation times. A faster relaxation mode at pH 9 attributed to a single polymer (i.e., a unimer with $R_h = 3.6$ nm) whereas the slower relaxation time at pH 3 to polymer aggregates with $R_h = 15.7$ nm. Considering the chemical structure of the block copolymer, the polymer aggregates may be expected to be a core−corona type micelle with protonated AaH blocks forming a core and charged NaAMPS blocks forming a corona layer. At pH 5, the relaxation time distribution was found to be bimodal with the fast and slow relaxation modes. The relaxation time for the fast mode is slightly faster than that at pH 9, indicative of a smaller unimer size at pH 5 because the AaH units are partially protonated. At pH 4.5 or lower, QELS distributions are unimodal corresponding to micelles. Remarkably, the R_h values for the polymer micelle decreased with decreasing pH from 5 to 3, presumably because at pH 5 the AaH units are partially deprotonated, and thus the AaH core may be swollen with water at this pH.

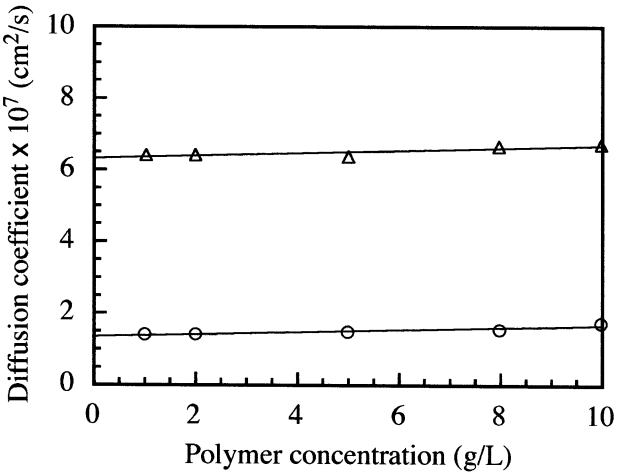

Figure 3. Concentration dependence of the diffusion coefficient of $pNaAMPS_{85}-AaH_{40}$ in 0.1 M NaCl aqueous solutions at pH 9 (△) and 3 (○) at $\theta = 90°$.

In general, D depends on C_p. The concentration dependence of D for $pNaAMPS_{85}-AaH_{40}$ at varying pH is shown in Figure 3. The concentration dependence of D is given by

$$D = D_0(1 + k_d C_p) \tag{4}$$

where D_0 is the infinite dilution diffusion coefficient and k_d is the diffusion second virial coefficient. The k_d is in part related to the hydrodynamic interactions in the solution by $k_d = 2A_2M_w - k_f - 2\nu_2$, where k_f is the concentration dependence of the friction coefficient and ν_2 is the partial specific volume of the solution. The dependences of D on C_p for the micelle at pH 3 and the unimer at pH 9 are very small; i.e., k_d values for the micelle at pH 3 and the unimers at pH 9 estimated from the plots in Figure 3 are 32.6 and 36.8 mL/g, respectively. Thus, apparent R_h values estimated at one finite concentration of the polymer ($C_p = 10$ g/L) in this study can be regarded as true R_h values.

Figure 4a compares variations of scattering intensities for solutions of the $pNaAMPS_{85}-AaH_{30}$ and $pNaAMPS_{85}-AaH_{40}$ diblock copolymers plotted against solution pH. The scattering intensities for both the polymers increase rapidly as the solution pH is decreased from 5 to 4, implying that micelles are formed at pH < 5. The scattering intensity corresponds to an increase in the micellar mass.

Figure 4b compares the intensity-average hydrodynamic radii ($\langle R_h \rangle$) as a function of pH. The symbol "$\langle\ \rangle$" is used because $\langle R_h \rangle$ is an average value of the fast and slow relaxation modes obtained from the ILT analysis. Above pH 5.5, the $\langle R_h \rangle$ values for $pNaAMPS_{85}-AaH_{30}$ and $pNaAMPS_{85}-AaH_{40}$ block copolymers are on the order of 2−3 nm, suggesting that the polymers are in

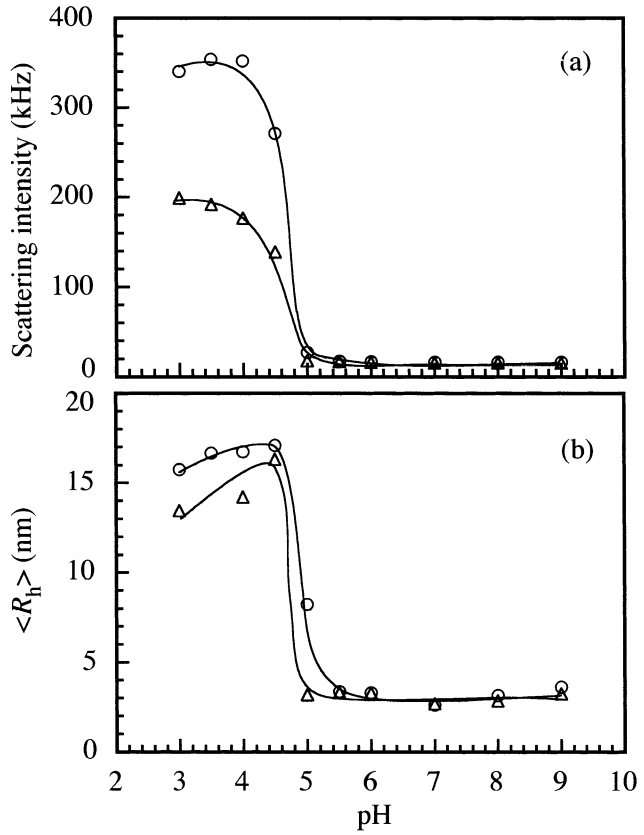

Figure 4. Scattering intensity (a) and intensity-average hydrodynamic radius ($\langle R_h \rangle$) (b) at $C_p = 10$ g/L for pNaAMPS$_{85}$−AaH$_{30}$ (△) and pNaAMPS$_{85}$−AaH$_{40}$ (○) as a function of pH in 0.1 M NaCl aqueous solutions at 25 °C.

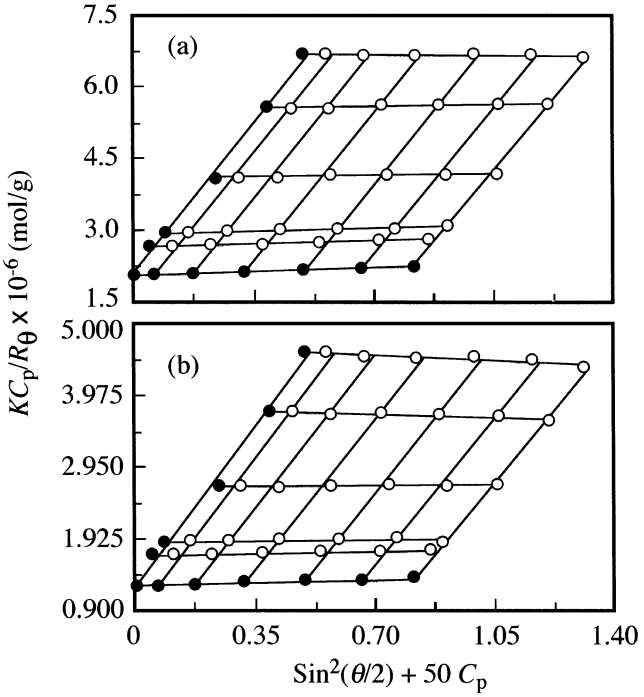

Figure 5. Zimm plots for pNaAMPS$_{85}$−AaH$_{30}$ (a) and pNaAMPS$_{85}$−AaH$_{40}$ (b) in 0.1 M NaCl at pH 3 at angles from 30° to 130° with a 20° increment. The polymer concentration was varied from 1.0 to 10 g/L. The Rayleigh ratio (R_θ) was determined by subtracting the solvent scattering from the total scattering of the solutions.

the state of unimers at pH > 5.5 in 0.1 M NaCl aqueous solutions. Upon decreasing pH, $\langle R_h \rangle$ values for pNaAMPS$_{85}$−AaH$_{30}$ and pNaAMPS$_{85}$−AaH$_{40}$ start to increase near pH 5 and 5.5, respectively, reaching maximum values near pH 4.5. These observations indicate the formation of polymer micelles at acidic pH's. The $\langle R_h \rangle$ values for the pNaAMPS$_{85}$−AaH$_{40}$ micelles at pH < 4.5 are slightly larger than those for the pNaAMPS$_{85}$−AaH$_{30}$ micelles. It should be noted here that the difference in the scattering intensities for the two block copolymer micelles (Figure 4a) is significantly larger than the difference in the $\langle R_h \rangle$ values. In other words, there seems to be a larger difference in the scattering intensities than in the $\langle R_h \rangle$ values between the two polymers. These observations suggest that the micellar masses or the aggregation numbers (N_{agg}) (i.e., the numbers of polymer chains included in one micelle) for the pNaAMPS$_{85}$−AaH$_{40}$ micelles are significantly larger than those for the pNaAMPS$_{85}$−AaH$_{30}$ micelles although the hydrodynamic sizes for the two block copolymer micelles are similar. We will discuss this point more in detail in the following subsection.

There is a tendency that the $\langle R_h \rangle$ values of the micelles decrease with decreasing pH below pH < 4.5. For example, the $\langle R_h \rangle$ value for the pNaAMPS$_{85}$−AaH$_{40}$ micelle decreased from 17.1 to 15.7 nm as the solution pH was decreased from 4.5 to 3, indicating that the polymer micelle becomes more compact due to further protonation of the carboxylate groups in the AaH block. A similar tendency has been reported on other associative polymers. For example, Armes and co-workers[22] reported that poly[ethylene oxide-*block*-2-(dimethylamino)ethyl methacrylate-*block*-2-(diethylamino)methacrylate] (PEO−DMA−DEA) triblock copolymers dissolve molecularly in acidic solution, but they form micelles above pH 7.3 comprising hydrophobic DEA cores, DMA inner shells, and PEO coronas; the hydrodynamic radius of the micelle decreased as the solution pH was increased from pH 7.3 to 9, the micelle becoming more compact due to the deprotonation of the tertiary amine residues in the DMA and DEA blocks.

Static Light Scattering (SLS). Zimm plots for the diblock copolymer micelles obtained by SLS measurements in 0.1 M NaCl aqueous solutions at pH 3 in the C_p range 1.0−10 g/L are shown in Figure 5. Values of dn/dC_p for the solutions of the pNaAMPS$_{85}$−AaH$_{30}$ and pNaAMPS$_{85}$−AaH$_{40}$ micelles at pH 3 were 0.162 and 0.164 mL/g, respectively. The SLS data for the diblock copolymer micelles at pH 3 are presented along with QELS data in Table 2. Values of M_w for the micelles were estimated by extrapolation of C_p and θ to zero, and values of R_g and A_2 were estimated from the slope of the angular and concentration dependence in the Zimm plots, respectively. A value of N_{agg} was calculated from the ratio of M_w values for the micelle and its unimer. M_w for the unimer was determined by GPC using a mixed solvent of water and acetonitrile (80/20, v/v) containing 0.1 M $NaNO_3$ as eluent. The M_w value, and thus N_{agg}, for the diblock copolymer micelle increases with increasing AaH block length. A decrease in the A_2 value observed for the micelle with increasing AaH block length is indicative of a decrease in the solubility (i.e., contraction) of the micelle with increasing length of the protonated AaH block. A similar trend in A_2 has been reported for poly(styrene-*block*-sodium acrylate) in aqueous solution; A_2 for poly(styrene-*block*-sodium acrylate) decreases with increasing the styrene block length.[23] The R_g value for the micelle is practically independent

Table 2. Quasi-Elastic and Static Light Scattering Data for Polymer Micelles Formed from the Diblock Copolymers at pH 3

sample code	M_w [a] $\times 10^{-5}$	A_2 [a] $\times 10^4$ (mol mL g^{-2})	R_g [a] (nm)	R_h [b] (nm)	R_g/R_h	N_{agg} [c]
pNaAMPS$_{85}$−AaH$_{30}$	4.85	2.27	17.2	13.5	1.27	13.2
pNaAMPS$_{85}$−AaH$_{40}$	7.99	1.61	17.2	15.7	1.10	20.5

[a] Determined by SLS in 0.1 M NaCl aqueous solutions. [b] Determined by QELS in 0.1 M NaCl aqueous solutions. [c] Apparent aggregation numbers of the diblock copolymer micelles calculated from M_w of the micelles determined by SLS in 0.1 M NaCl at pH 3 and M_w of the corresponding unimers determined by GPC eluted with a mixed solvent of water and acetonitrile (80/20, v/v) containing 0.1 M $NaNO_3$.

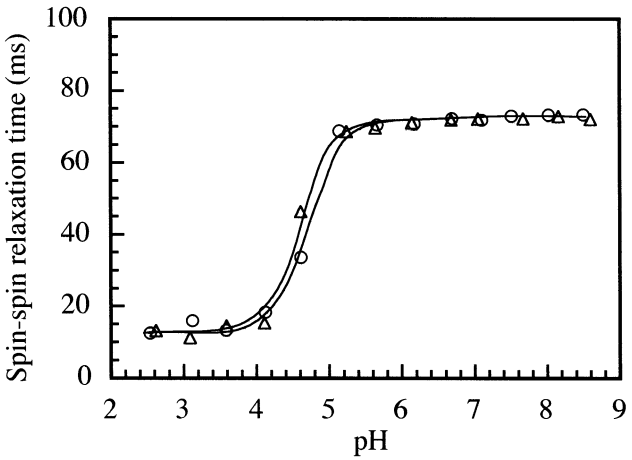

Figure 6. Spin−spin relaxation time (T_2) for pNaAMPS$_{85}$−AaH$_{30}$ (△) and pNaAMPS$_{85}$−AaH$_{40}$ (○) as a function of pH in D_2O containing 0.1 M NaCl at C_p = 10 g/L.

of the length of the AaH block (Table 2). The R_g/R_h ratio is a parameter that depends on the polymer chain conformation and polydispersity. The theoretical value of the R_g/R_h ratio for a homogeneous sphere is 0.778, and it increases substantially for a less dense structure and polydisperse solution.[24−27] The R_g/R_h ratios for pNaAMPS$_{85}$−AaH$_{30}$ and pNaAMPS$_{85}$−AaH$_{40}$ micelles are 1.27 and 1.10, respectively. This observation suggests that the protonated AaH block core of pNaAMPS$_{85}$−AaH$_{40}$ is more dense than that of pNaAMPS$_{85}$−AaH$_{30}$ in 0.1 M NaCl aqueous solution at pH 3.

^{1}H NMR Relaxation Times. ^{1}H NMR relaxation times are influenced by changes in the dynamic motion of protons. Spin−spin relaxation time (T_2) decreases as the molecular motion decreases. To obtain information about motional restriction of the pendent alkyl chains in the AaH block when the polymers form micelles, we performed ^{1}H NMR relaxation time measurements with the diblock copolymers in D_2O containing 0.1 M NaCl under various pH conditions. In Figure 6, T_2 values for the two diblock copolymers observed at δ = 1.32 ppm associated with the methylene protons in the pendent alkyl chains of AaH blocks are plotted against pH. At pH > 5, the T_2 values for pNaAMPS$_{85}$−AaH$_{40}$ and pNaAMPS$_{85}$−AaH$_{30}$ are virtually constant at 74 ms. Upon decrease in pH from 5 to 4, T_2 values sharply decrease, reaching a constant value of 13 ms. These observations indicate that transitions from unimer to micelle, and vice versa, occur within a narrow range of pH between 4 and 5. As far as the T_2 values tell about the motional freedom of the pendent alkyl groups in the AaH block, there seems to be little or no difference between the two block copolymers with different lengths of the AaH blocks for both the unimer and micellar states.

Fluorescence. The fluorescence spectra of the ANS probe indicate the microscopic polarity around the

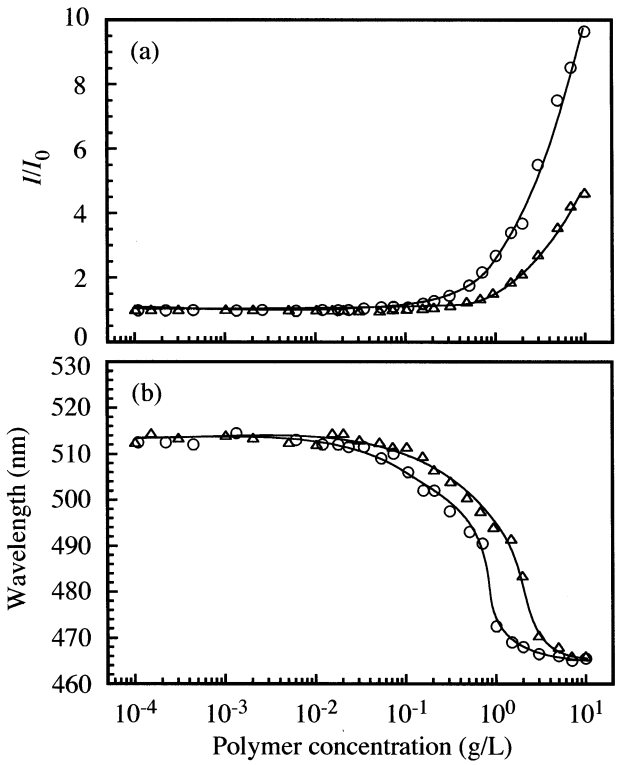

Figure 7. Relative fluorescence intensity (I/I_0) (a) and wavelength of emission maximum (b) in ANS (1.89×10^{-4} M) fluorescence spectra as a function of C_p for pNaAMPS$_{85}$−AaH$_{30}$ (△) and pNaAMPS$_{85}$−AaH$_{40}$ (○) in 0.1 M NaCl aqueous solutions at pH 3.

probe.[28−31] ANS emits fluorescence strongly in nonpolar media accompanying a significant blue shift while it emits weakly in polar media. Therefore, an increased fluorescence intensity along with a blue shift of the emission maximum indicates that the probe is located in less polar media. It is also known that fluorescence intensity and emission maximum are not influenced by changes in pH between 2 and 11.[32]

In Figure 7a, the relative fluorescence intensity (I/I_0) in ANS fluorescence spectra for ANS (1.89×10^{-4} M) solubilized in 0.1 M NaCl aqueous solutions at pH 3 in the presence of the diblock copolymers are plotted against C_p, where I and I_0 are the fluorescence intensities in the presence and absence of the diblock copolymers, respectively. At pH 3, the I/I_0 ratios in the presence of pNaAMPS$_{85}$−AaH$_{40}$ and pNaAMPS$_{85}$−AaH$_{30}$ are around 1 at C_p < 0.1 and 0.5 g/L, respectively. As C_p is increased, the I/I_0 ratios for the block copolymers commence to increase near C_p = 0.1 and 0.5 g/L, respectively. These observations suggest that the diblock copolymer micelles are able to incorporate ANS molecules into a hydrophobic environment formed from the association of the AaH blocks. For the diblock copolymer with a longer AaH chain, the onset for the increase in the I/I_0 ratio seems to shift toward lower C_p, indicating

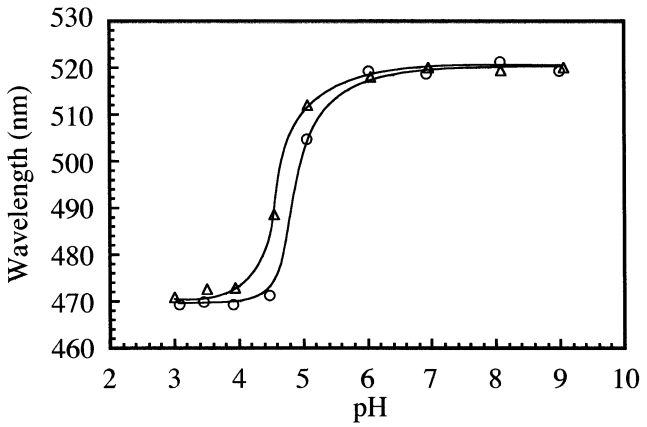

Figure 8. Wavelength of emission maximum in ANS (1.89×10^{-4} M) fluorescence spectra as a function of pH in the presence of pNaAMPS$_{85}$−AaH$_{30}$ (△) and pNaAMPS$_{85}$−AaH$_{40}$ (○) at $C_p = 5.0$ g/L in 0.1 M NaCl aqueous solutions.

that hydrophobic associations occur at lower C_p with increasing the length of the AaH block.

In Figure 7b, the emission maximum wavelength for the ANS fluorescence in the presence of the diblock copolymer is plotted against C_p. The maximum wavelength in the presence of the diblock copolymers is constant at 513 nm in a lower C_p region, but the emission maximum wavelength for pNaAMPS$_{85}$−AaH$_{40}$ and pNaAMPS$_{85}$−AaH$_{30}$ begins to decrease in the C_p region 0.005−0.05 g/L with increasing C_p, reaching a blue-shifted wavelength of about 465 nm at higher C_p. This blue shift suggests that hydrophobic domains are formed when C_p is higher than a certain level, in which ANS probes are solubilized. Although the data in Figure 6a,b suggest the presence of a critical micelle concentration (cmc), we were unable to determine cmc because the onset for the increase in the I/I_0 ratio, and the decrease in the emission maximum wavelength was not well-defined. The increase in the I/I_0 ratio (Figure 7a) and the decrease in the emission maximum at $C_p >$ cmc (Figure 7b) reflect an increase in the number of the micelles with an increase in C_p.

In Figure 8, the emission maximum wavelength for ANS solubilized in 0.1 M NaCl aqueous solutions in the presence of the diblock copolymers at $C_p = 5.0$ g/L is plotted against pH. In a high-pH region (pH ≥ 6), the emission maximum is practically constant at 518 nm, which is almost the same as that for ANS in water. At pH < 6, however, the emission maximum blue shifts to 470 nm with decreasing pH within a pH range of 6−4. A pH value for the onset of the blue shift is slightly higher for the pNaAMPS$_{85}$−AaH$_{40}$ micelle than for the pNaAMPS$_{85}$−AaH$_{30}$ micelle. These observations agree well with the observations in ^{1}H NMR relaxation times (Figure 6). When pH was decreased from 9 to 3 and subsequently increased back to 9, pH-induced fluorescence spectral changes were found to be completely reversible without hysteresis.

In an earlier paper, we reported pH-induced self-association behavior of a random copolymer of NaAMPS and 50 mol % of sodium 11-acrylamidoundecanoate prepared by ordinary free-radical polymerization.[33,34] This random copolymer in aqueous solution was proven to exist as an open chain under basic conditions and as a unimolecular micelle under acidic conditions, and thus a conformational change from an open chain to unimolecular micelle is induced by pH. The both the block and random copolymers exist as unimers at basic pH's and form micelles at acidic pH's. However, the types of the micelles formed from the block and random copolymers are completely different: unimolecular micelles in the case of the random copolymer while multipolymeric micelles in the case of the block copolymers. The pH-induced transitions from unimers to micelles, and vice versa, are completely reversible without hysteresis for both the random and block copolymers.

Conclusions

The diblock copolymers of NaAMPS and AaH were synthesized via RAFT polymerization. The polymerization of AaH used by NaAMPS macro-CTA proceeded in accordance with a "living" mechanism that was confirmed by the fact that M_n increased linearly with the conversion of the monomer. The molecular weight distributions for the obtained diblock copolymers were narrow ($M_w/M_n \leq 1.32$). The pH-induced association behavior of the diblock copolymers in 0.1 M NaCl aqueous solutions was preliminarily investigated by QELS, SLS, ^{1}H NMR relaxation, and fluorescence probe techniques. These experimental data indicated that the diblock copolymers formed polymer micelles in 0.1 M NaCl aqueous solutions at low pH's whereas the micelle was dissociated at high pH's. pH-induced association and dissociation were found to be completely reversible without hysteresis. Longer AaH block lengths lead to increased N_{agg} for the micelles. We believe the RAFT process will became one of the most important methods to synthesize well-defined water-soluble polymers.

References and Notes

(1) Hurter, P. N.; Hatton, T. A. *Langmuir* **1992**, *8*, 5300.
(2) Kataoka, K.; Kwon, G. S.; Yokoyama, M.; Okano, T.; Sakurai, Y. *J. Controlled Release* **1993**, *24*, 119.
(3) Topp, M. D. C.; Dijkstra, P. J.; Talsma, H.; Feijen, J. *Macromolecules* **1997**, *30*, 8518.
(4) Bütün, V.; Armes, S. P.; Billingham, N. C.; Tuzar, Z.; Rankin, A.; Eastone, J.; Heenan, R. K. *Macromolecules* **2001**, *34*, 1503.
(5) Paz Bañez, M. V.; Robinson, K. L. Bütün, V.; Armes, S. P. *Polymer* **2001**, *42*, 29.
(6) Georges, M. K.; Veregin, P. M.; Kazmaier, P. M.; Hamer, G. K. *Macromolecules* **1993**, *26*, 2987.
(7) Kato, M.; Kamigaito, M.; Sawamoto, M.; Higashimura, T. *Macromolecules* **1995**, *28*, 1721.
(8) Wang, J.-S.; Matyjaszewski, K. *Macromolecules* **1995**, *28*, 7572.
(9) Chiefari, J.; Chong, Y. K.; Ercole, F.; Krstina, J.; Le, T. P.; Mayadunne, R. T. A.; Meijs, G. F.; Moad, G.; Moad, C. L.; Rizzardo, E.; Thang, S. H. *Macromolecules* **1998**, *31*, 5559.
(10) Arotçaréna, M.; Heise, B.; Ishaya, S.; Laschewsky, A. *J. Am. Chem. Soc.* **2002**, *124*, 3787.
(11) Mitsukami, Y.; Donovan, M. S.; Lowe, A. B.; McCormick, C. L. *Macromolecules* **2001**, *34*, 2248.
(12) Gabaston, L. I.; Furlong, S. A.; Jackson, R. A.; Armes, S. P. *Polymer* **1999**, *40*, 4504.
(13) Shibaev, V. P.; Platé, N. A.; Freidzon, Y. S. *J. Polym. Sci., Polym. Chem. Ed.* **1979**, *17*, 1655.
(14) Jakes, J. *Czech. J. Phys.* **1988**, *B38*, 1035.
(15) Brown, W.; Nicolai, T.; Hvidt, S.; Stepanek, P. *Macromolecules* **1990**, *23*, 375.
(16) Zimm, B. H. *J. Chem. Phys.* **1948**, *16*, 1099.
(17) Meiboom, S.; Gill, D. *Rev. Sci. Instrum.* **1958**, *29*, 688.
(18) Mikkelsen, K.; Nielsen, S. O. *J. Phys. Chem.* **1960**, *64*, 632.
(19) Sumerlin, B. S.; Donovan, M. S.; Mitsukami, Y.; Lowe, A. B.; McCormick, C. L. *Macromolecules* **2001**, *34*, 6561.
(20) Donovan, M. S.; Sanford, T. A.; Lowe, A. B.; Sumerlin, B. S.; Mitsukami, Y.; McCormick, C. L. *Macromolecules* **2002**, *35*, 4570.
(21) Donovan, M. S.; Lowe, A. B.; Sumerlin, B. S.; McCormick, C. L. *Macromolecules* **2002**, *35*, 4123.
(22) Liu, S.; Weaver, J. V. M.; Tang, Y.; Billingham, N. C.; Armes, S. P.; Tribe, K. *Macromolecules* **2002**, *35*, 6121.

(23) Khougaz, K.; Astafieva, I.; Eisenberg, A. *Macromolecules* **1995**, *28*, 7135.
(24) Qin, A.; Tian, M.; Ramireddy, D.; Webber, S. E.; Munk, P.; Tuzar, Z. *Macromolecules* **1994**, *27*, 120.
(25) Nordmeier, E.; Lechner, M. D. *Polym. J.* **1989**, *21*, 623.
(26) Mössmer, S.; Spatz, J. P.; Möller, M.; Aberle, T.; Schmidt, J.; Burchard, W. *Macromolecules* **2000**, *33*, 4791.
(27) Konishi, T.; Yoshizaki, T.; Yamakawa, H. *Macromolecules* **1991**, *24*, 5614.
(28) Slavik, J. *Biochim. Biophys. Acta.* **1982**, *694*, 1.
(29) Humit, A. H.; Jirgensons, B. *Biochemistry* **1973**, *12*, 1609.
(30) Weber, G.; Young, L. B. *J. Biol. Chem.* **1976**, *106*, 497.
(31) Stryer, L. *J. Mol. Biol.* **1965**, *13*, 482.
(32) Penzer, G. R. *Eur. J. Biochem.* **1972**, *25*, 218.
(33) Yusa, S.; Sakakibara, A.; Yamamoto, T.; Morishima, Y. *Macromolecules* **2002**, *35*, 5243.
(34) Yusa, S.; Sakakibara, A.; Yamamoto, T.; Morishima, Y. *Macromolecules* **2002**, *35*, 10182.

MA030065X